http://ansinet.com/itj

ITJ

ISSN 1812-5638

INFORMATION TECHNOLOGY JOURNAL

ANSInet
Asian Network for Scientific Information
308 Lasani Town, Sargodha Road, Faisalabad - Pakistan

Information Technology Journal 12 (17): 4019-4025, 2013
ISSN 1812-5638 / DOI: 10.3923/itj.2013.4019.4025

Analysis on NLOS Channel Modeling on Airport Surface Surveillance

Gong Fengxun and Ma Yanqiu
College of Electronic and Information Engineering, Civil Aviation University of China, Tianjin, China

Abstract: The channel model has been established by analyzing the characteristics of the non-line-of-sight environment in a domestic airport surface and referencing mobile communication and air channel research. Through estimating the channel multipath time delay and deducing the analytical formula of Doppler spectrum that incident angle in Gaussian distribution, we got the spread of frequency that produced by relative motion and we describe the relevance of the established channel by contrasting the actual value and theoretical value of the channel correlation coefficient. Channel evaluation also by analyzing channel capacity in different antenna configuration to compare priori knowledge. The simulation results show that the established channel model can accurately describe the characteristics of the non-line-of-sight environment in the airport surface and it can be used for the design of multilateration (MLAT) system and the research of Time Difference of Arrival (TDOA) localization algorithm.

Key words: NLOS, GDOP, channel modelling, multilateration (MLAT), TDOA

INTRODUCTION

For improving the positioning precision of MLAT system, it must solve the NLOS problem. The NLOS environment between the Mobile Station (MS) and Base Station (BS) can make excess delay of TDOA value, namely NLOS error. It can't eliminate NLOS error by improving the system of the measuring accuracy of TDOA receiver. In order to reduce positioning blind spot the Capital Airport has increased the number of base stations from 15 to 26 and then increased to 37. The relevant data show that the classic positioning algorithms are difficult to meet the precise positioning requirements. In 2001 Mcgurie proposed the method that uses the observation data reprocessing extract the transmission delay to locate the moving target (Mcguire *et al*., 2001). In 2004 Xie Hong proposed that estimated the NLOS mean error according to the prior information of the channel and the Greenstein model (Xie *et al*., 2006). The international analysis of NLOS error has gradually from estimating the measured data to estimating the channel characteristics. Constructing non-line-of-sight channel model for terminal area at low altitude has great significance to improve the accuracy of the positioning system.

The research on aviation channel especially NLOS channel suitable for airport surface at home and abroad is less than on wireless channel. In the aviation channel aspect, (Bello, 1973) analysis the characteristics of air channel. The authors do some improvement and implementation to the aviation channel statistical model based on the incident angle in (Zhu *et al*., 2009). In (Pan *et al*., 2011), a mixed application channel model about aviation and wireless communication is proposed; the model is used to simulate various fading signal. It analysis the Unmanned Air Vehicle (UAV) in different flight status, proposed a statistical channel model that is applied to UAV in (Tan and Zhang, 2010). The interference between channels caused by multi-path and multiple antenna transceiver situations are introduced in (Gong *et al*., 2011) and (Miao *et al*., 2007). The channels of above are all include LOS component and has not test whether the channel applicable. Referencing the channel model of above and anglicizing the real NLOS airport surface environment, also combining with MLAT technology, a channel model is proposed and evalua-ted in this study. We evaluated the channel from the respects those include multipath delay estimation, Doppler power spectrum, the correlativity of the channel and channel capacity. The simulation results show that the established channel model can effectively inhibit the excess delay and improve the precision of the MLAT positioning system.

ESTABLISHING CHANNEL MODEL ACCORDING TO THE ACTUAL ENVIRONMENT

The description of actual airport surface environment: Multiple antenna communication combines antenna diversity and space-time code technology which can effective against multipath fading and improve spectrum efficiency. The research about multiple antenna

Corresponding Author: Gong Fengxun, College of Electronic and Information Engineering, Civil Aviation University of China, Tianjin, China

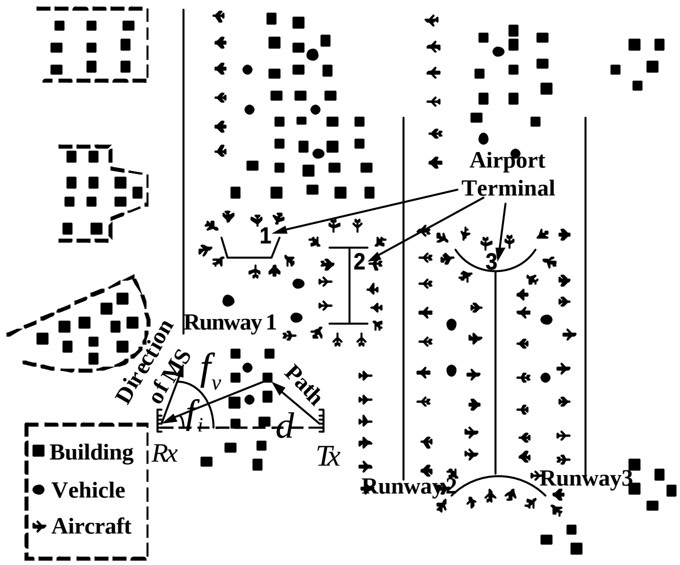

Fig. 1: The schematic diagram of an airport surface

technology applied in aviation channel has started in recent years (Jensen *et al*., 2007).

A domestic airport surface environment is shown in Fig. 1. Scattering environment between the transmitting antenna array and target receiving antenna array is made up of ground building vehicles and landing or take-off aircraft. The distance from MS to BS is d.

Taking a single transmission path for example, we assume that the movement direction of MS is ϕ_v. Signal will arrive at the target receiving antenna array in angle ϕ_v after reflection, diffraction or scattering of the scattering environment.

Calculate the channel fading coefficient matrix β: We can get a symmetrical mapped matrix Cfrom

$$R = CC^T \quad (1)$$

And then we can calculate the channel fading coefficient matrix $\beta^l$of the l path:

$$vec(\beta^l) = \sqrt{P_l} Ca_l \quad (2)$$

vec(.) makes matrix to vector. α_l indicates mean 0 and variance 1 independent identically distributed plural Gaussian variables. P_l is the average power gain of path l.

Constructed the Channel Matrix: According to the above step to get each parameter we can get channel matrix H by Eq. 2.

MULTIPATH DELAY ESTIMATION AND DOPPLER POWER SPECTRUM

Multipath delay estimation: The multipath delay estimation of the channel takes full advantage of the signal's time-frequency characteristics. In the time domain, we use the related technology to detect the reception signal and do a rough estimate. In the frequency domain, we do the FFT transform for the received signal in the maximum correlation value corresponding moment and we do the accurate estimate by obtaining the phase offset caused by the delay. Both the use of the relevant anti-noise characteristics and the high precision of the phase method we greatly improved the accuracy of the delay estimation.

We assume that the transmitted signal is x(t), the target received signal is y(t). To facilitate the derivation, the received signal abbreviated as:

$$y(t) = \beta x(t-\tau_l)+n \quad (3)$$

Rough estimate in time domain: Sampling the received signal by $T_s = T/N$, then:

$$Y(kT_s) = \beta x(kT_s-\tau_f)+n(kT_s) \quad (4)$$

τ_f is less than a sampling interval so it is called the fractional delay.

Correlating the sampled signal with the local sequence:

$$R(m)=\sum_{k=0}^{N-1} y_{k+m}\cdot x_k^* \tag{5}$$

y_k is a discrete sampling of the received signal, x_k is the sample sequence of the transmitted signal.
$\hat{d}$ is the sample number corresponding to the maximum correlation value. And:

$$\hat{d}=\arg\left\{\max_m |R(m)|\right\} \tag{6}$$

Then, the integer delay is:

$$\hat{\tau}_c=\hat{d}\cdot T_s \tag{7}$$

Accurate estimate in frequency domain: After the rough estimate we do FFT transform for the received data, we can get frequency data Y_i. $Z_i=Y_i\cdot X_i^*$ in which X_i is the transmission data of the frequency domain, i = 0, 1,…,N-1:

$$W=\sum_{i=0}^{N-\Delta-1} Z_{i+\Delta}\cdot Z_i^* \tag{8}$$

The phase of W is $\hat{\varphi}=\text{angle}\{W\}$ in which $\hat{\varphi}$ is the estimated value of the phase shift difference between the Δ subcarriers.

Because the fractional delay lead to the phase offset of the frequency domain data, the data on the subcarrier i corresponds to the phase offset of the transmission data is:

$$\theta_i=2\pi\frac{i}{T}\tau_f \tag{9}$$

The difference of phase shift between subcarrier i+Δ and subcarrier i is:

$$\theta_{i+\Delta}-\theta_i=2\pi\frac{i+\Delta}{T}\tau_f-2\pi\frac{i}{T}\tau_f=2\pi\frac{\Delta}{T}\tau_f \tag{10}$$

Combined with $\hat{\varphi}$ we get the fractional delay is:

$$\hat{\tau}_f=\frac{\hat{\varphi}}{2\pi\Delta/T} \tag{11}$$

We suppose that during the reception the inherent delay is τ', then the actual delay estimation value is:

$$\tau_l=\hat{\tau}_c+\hat{\tau}_f-\tau' \tag{12}$$

The derivation of doppler power spectrum: We suppose the speed of MS is v and carrier frequency $f_c=c/\lambda$. Figure 1 shows that the movement direction of MS is ϕ_v. The Doppler frequency of path l can be written as:

$$f_i=f_d\cos(\phi_i-\phi_v)+f_c \tag{13}$$

The maximum Doppler frequency shift is f_d. Angle of arrive ϕ_i is:

$$\phi_i=\phi_v\pm\arccos\left|\frac{f_i-f_c}{f_d}\right|,\ \phi_i \gtrless \phi_v \tag{14}$$

The number of incident wave is N_s, the probability density function (PDF) of the incident wave angle distribution is $p(\phi)$.$p(\phi)d\phi$ denotes the energy when the incident angle belongs to $[\phi,\phi+d\phi]$.

When the scattering distributed very intensive, $p(\phi)d\phi$ is close to continuous distribution. We use ϕ instead of ϕ_i, f instead of f_i. After derivation of Eq. 14, we get:

$$df=-f_d\sin(\phi-\phi_v)d\phi \tag{15}$$

And from Eq.14, there is:

$$\sin(\phi-\phi_v)=\sqrt{1-\left(\frac{f-f_c}{f_d}\right)^2} \tag{16}$$

We use S(f) denotes the Doppler spectrum. Then:

$$S(f)df=A[G(\phi)p(\phi)+G(-\phi)p(-\phi)]d\phi \tag{17}$$

A denotes the average receive power of the Omni-directional antenna. The antenna gain of direction ϕ is $G(\phi)$. We suppose antenna gain $G(\phi)$ is constant on Omni-directional, namely $G(\phi)=1$. From 14, 15, 16 and Eq. 17 we get the complete expression of Doppler spectrum:

$$S(f)=\frac{A[G(\phi)p(\phi)+G(-\phi)p(-\phi)]}{f_d\sqrt{1-\left(\frac{f-f_c}{f_d}\right)^2}}=\frac{p\left(\phi_v+\arccos\left(\frac{f-f_c}{f_d}\right)\right)+p\left(\phi_v-\arccos\left(\frac{f-f_c}{f_d}\right)\right)}{f_d\sqrt{1-\left(\frac{f-f_c}{f_d}\right)^2}},\quad |f-f_c|<f_d \tag{18}$$

For the convenience of the following derivation, we define:

$$\phi_f=\arccos\left(\frac{f-f_c}{f_d}\right),\ 0\le\phi_f\le\pi \tag{19}$$

The airport usually located in remote areas and suburban environment and Gauss model is more practical than the uniform model. When the incident angle obeys Gauss distribution, its Standard deviation is σ and the PDF is:

$$p(\phi) = K\exp\left(-\frac{(\phi-\phi_0)^2}{2\sigma^2}\right)/(\sqrt{2\pi}\sigma); \qquad -\pi+\phi_0 \le \phi \le \pi+\phi_0 \tag{20}$$

k denotes normalization coefficient and deduces that $K = 1/\mathrm{erf}(\pi/\sqrt{2}\sigma)$ while erf(.) is error function. Bring Eq. 20 to 18, we get:

$$S(f) = \frac{K}{\sqrt{2\pi}\sigma \cdot f_d\sqrt{1-(\frac{f-f_c}{f_d})^2}} \left\{\exp\left[-\frac{(\phi_v+\phi_f-\phi_0)^2}{2\sigma^2}\right] + \exp\left[-\frac{(\phi_v-\phi_f-\phi_0)^2}{2\sigma^2}\right]\right\} \qquad |f-f_c| < f_d \tag{21}$$

SIMULATION RESULTS WITH ANALYSIS

In order to evaluate the established channel model in this study, we did six kinds of simulation as below. The general parameters of the simulation include the carrier frequency 2 GHz and the speed of MS 200 km/h.

Simulation of doppler power spectrum: Suppose the incident wave obeys the Gaussian distribution, average incident angle $\phi_0 = 0°$ and the movement direction of the target is 0°, 90° and 180°. We get the Doppler spectrum in different direction as follows.

Figure 2 shows that when the movement direction is 0°, MS move towards BS. When σ is small, it means the incident expansion angle is small.

At this time the scatterer are mainly distributed between the MS and BS and the power spectrum energy is mainly distributed in the positive frequency shift. AS σ becomes bigger, the incident expansion angle becomes bigger. So the scatterer behind BS increases as the energy in the negative frequency shift gradually increases.

Figure 3 shows that when the movement direction is 90°, MS moves perpendicular to the connection between MS and BS. When σ is small, the scattering object are relatively concentrated near the average incidence angle. Small frequencies shift have larger energy while large frequencies shift with less energy. AS σ becomes bigger, scattering distribution tends to be uniform distribution of [-π, π] and power spectrum approaches to the classic spectrum.

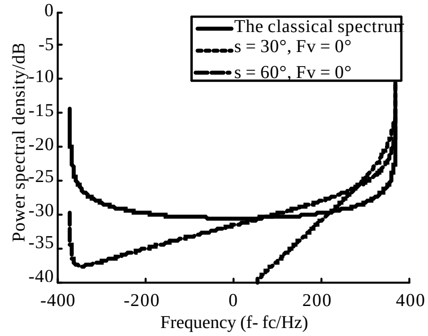

Fig. 2: $\phi_v = 0°$

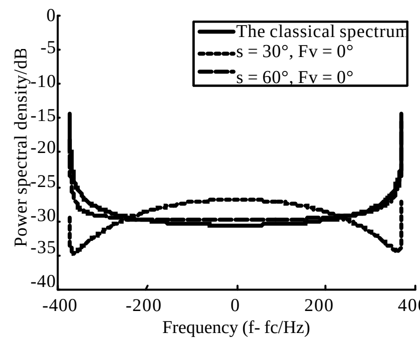

Fig. 3: $\phi_v = 90°$

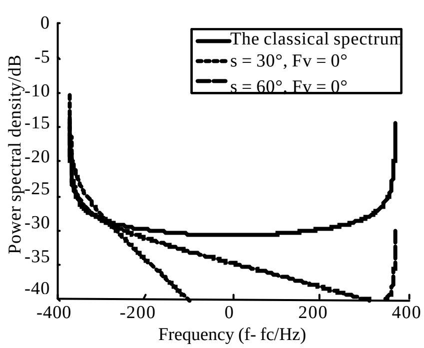

Fig. 4: $\phi_v = 180°$

Figure 4 tells that when the movement direction is 180°, MS deviate from BS. The Doppler power spectrum is mainly concentrated in the negative half shaft.

Simulation of bit error rate (BER): Rayleigh channel is a commonly used NLOS channel. We calculate the BER of our channel and compare it to the Rayleigh channel and the channel in (Pan *et al*., 2011). The result is shown in Fig. 5.

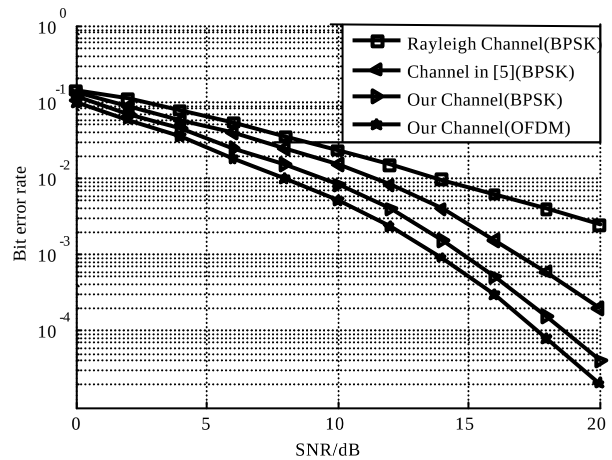

Fig. 5: The comparison of different channels

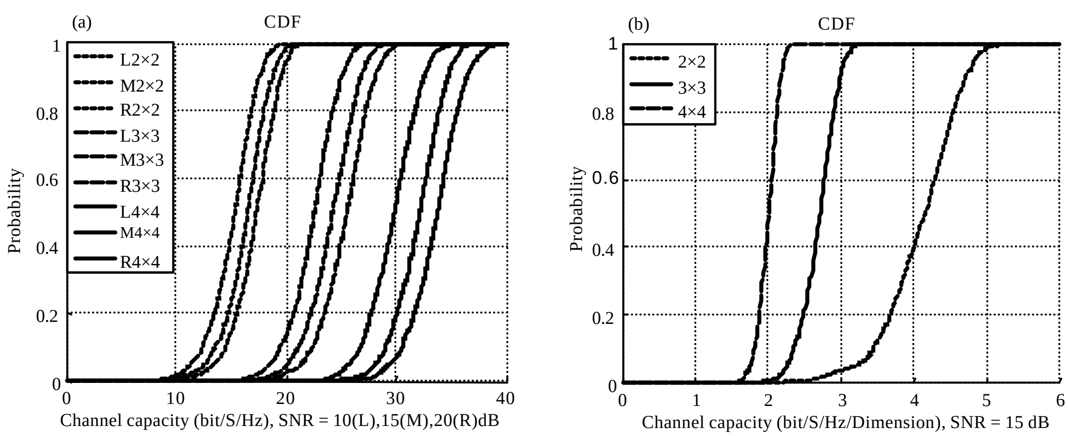

Fig. 6: The CDF of channel capacity (a) Total channel capacity and (b) Channel capacity per dimension

our channel is small than the Rayleigh channel and the channel in (Pan *et al.*, 2011), so our channel has good communication performance and suitable for the analysis of NLOS environment. And we also see that the OFDM modulation has lower BER than the BPSK modulation.

Simulation of cumulative distribution function (CDF) of channel capacity: The comparison of the total channel capacity and the channel capacity per dimension in different antenna configuration is shown in Fig. 6. The different antenna configuration is 2×2, 3×3 and 4×4.

From Fig. 6, the channel capacity increases as the SNR increases. As the number of antenna increases, the total channel capacity increases while the channel capacity per dimension decreases. Because the more the number of antenna is, the larger the mutual correlation of each antenna becomes. It makes the rank of the channel transfer function matrix with additional loss and finally leads to the drop of the channel capacity per dimension. This result is the same as Fig. 12 in (Czink *et al.*, 2007; Greenstein *et al.*, 1997; Yu *et al.*, 2004). So our channel coincides with the priori knowledge.

Spatial correlation coefficient of the channel: Take the 2×2 antenna configuration for example and we choose the environment that there is no direct propagation path between the base station and the target. Figure 7 shows the correlation coefficient between each transceiver antenna and the first transceiver antenna in four different paths. (1, 2) indicates antenna pairs that consist of the first receiving antenna and the second transmitting antenna, other and so on. The dashed line represents the actual spatial correlation coefficient in which the value of the channel correlation matrix is obtained by environmental parameters. The solid line represents the spatial correlation coefficient obtained by simulation

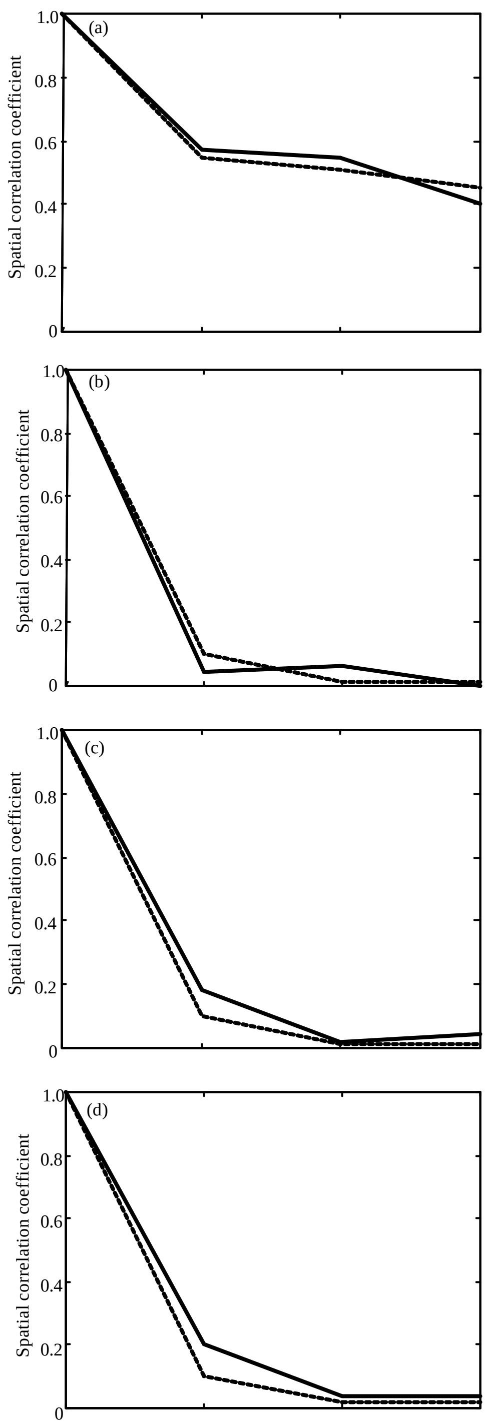

Fig. 7(a-d): The Spatial Correlation Coefficient in Different Path (a) The Spatial Correlation Coefficient of the First Path (b) The Spatial Correlation Coefficient of the Second Path (c) The Spatial Correlation Coefficient of the Third Path and (d) The Spatial Correlation Coefficient of the Forth Path

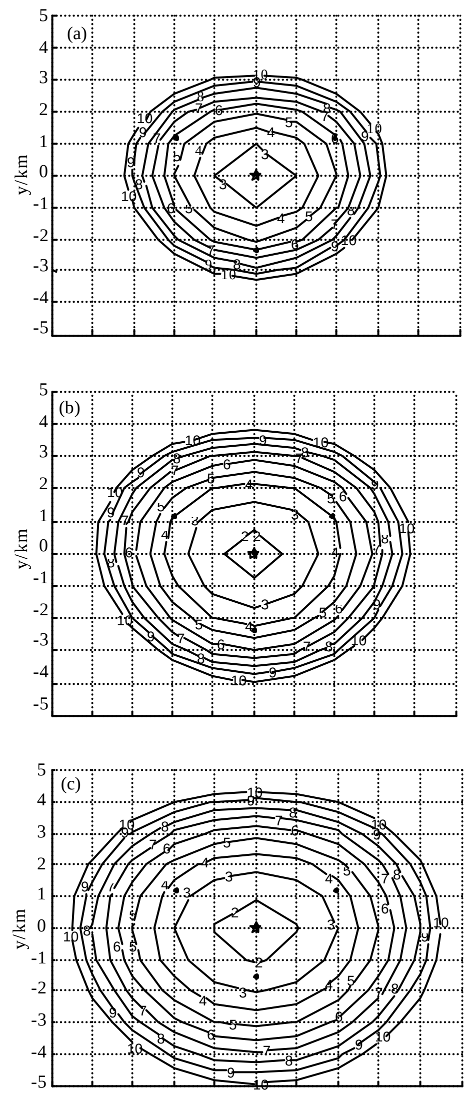

Fig. 8(a-c): The GDOP contour line in different channels (a) Rayleigh channel (b) The channel in Refer (Pan *et al*., 2011) and (c) Our design channels

which is obtained by calculating the correlation coefficient between the individual elements in the channel matrix. We can see that the error between the actually obtained spatial correlation coefficient and the theoretical value is smaller.

Simulation of geometric dilution of precision (GDOP) in different channels: We suppose the height of the target is 2km and use the Star-model Station. Then we get the coverage of positioning precision in different channels as below in Fig. 8.

Different channels produce different TDOA error that decline the precision of the location algorithm. We get the

GDOP contour line with the same embattling mode. From Fig. 8, the positioning coverage of our channel is larger than the Rayleigh channel and the channel in References (Pan *et al*., 2011). So our channel is suitable for the analysis of location algorithm.

CONCLUSIONS

Establishment of NLOS propagation channel model that conforms to the real environment has important significance for improving the precision of the positioning system. According to the NLOS problem in MLAT system, a channel model is proposed after the analysis of the real airport surface environment. Firstly, the established channel is based on the distribution of the scattering object and the construction method is clear. Secondly, simulations and the analysis show that the model is suitable for NLOS environment and it can well describe the condition of Doppler frequency shift caused by relative motion. It has good communication performance and the increase or decrease trend of channel capacity in different antenna configuration coincide with the prior knowledge. And it can be used for the design of MLAT system and the research of TDOA localization algorithm. Finally, we can select the appropriate parameters to make the channel widely used in a variety of typical wireless communication environment of low-altitude terminal area.

ACKNOWLEDGMENT

The authors wish to thank the anonymous referees for their careful review and detailed comments that helped to improve the readability and contents of the study. This work is financially supported by the National Natural Science Foundation of China (No. 61079008, U1233112), the Application Basis and Front Technology of Tianjin (No. 11JC2DJC25200) and Fundamental Research Funds for The Central Universities (No. ZXH2011B001; ZXH2011D011).

REFERENCES

Gong, F., Y. Lei and Y. Ma, 2011. Surface surveillance system of main station off-center and performance analysis. J. Xidian Univ., 38: 173-179.

Yu, K., M. Bengtsson, B. Ottersten, D. McNamara, P. Karlsson and M. Beach, 2004. Modeling of wide-band MIMO radio channels based on NLOS indoor measurements. Trans. Veh. Technol., 53: 655-665.

Greenstein, L.J., V. Erceg, Y.S. Yeh and M.V. Clark, 1997. A new path-gain/delay-spread propagation model for digital cellular channels. Trans. Veh. Technol., 46: 477-485.

Jensen, M.A., M.D. Rice and A.L. Anderson, 2007. Aeronautical telemetry using multiple-antenna transmitters. Trans. Aerospace Elect. Syst., 43: 262-272.

Mcguire, M., K. Plataniotis and A.N. Venetsanopoulos, 2001. Estimating position of mobile terminals from delay measurements with survey data. Proceedings of the Canadian Conference on Electrical and Computer Engineering, Volume 1. May 13-16, 2001, Toronto, Ont., pp: 129-134.

Miao, H., K. Yu and M.J. Juntti, 2007. Positioning for NLOS propagation: Algorithm derivations and cramer-rao bounds. Trans. Veh. Technol., 56: 2568-2580.

Czink, N., A. Richter, E. Bonek, J.P. Nuutinen and J. Ylitalo, 2007. Including diffuse multipath parameters in MIMO channel models. Proceedings of the 66th International Conference on Vehicular Technology, Volume 66, September 30-October 3, 2007, Baltimore, MD., pp: 874-878.

Bello, P.A., 1973. Aeronautical channel characterization. Trans. Commun., 21: 548-563.

Pan, Q.H., L.M. Zhao and M. Xu, 2011. The analysis and simulation of fading hybrid applications for aeronautical radio channel. Comput. Simul., 28: 52-52.

Zhu, Q.M., D.Z. Xu, W.H. Lu and X. Chen, 2009. Modified stochastic model of aeronautical channel. J. Applied Sci., 27: 569-573.

Xie, H. and N. Wei, 2006. A simplified non-line-of-sight error suppression algorithm based on TDOA. Harbin Eng. Univ., 26: 114-118..

Tan, Z. and X.L. Zhang, 2010. Modeling and performance analysis of multiple-antennae communication channel for pilotless helicopter. J. Beijing Univ. Aeronaut. Astronaut., 36: 1171-1175.